euspen's 26th International Conference & Exhibition, Krakow, PL, June 2026
www.euspen.eu

FEA-Informed Compensation of Thermal Volumetric Effects on Machine Structure

Daniel Divíšek [1], Martin Mareš [1], Otakar Horejš [1], Matěj Sulitka [1]

[1] *Czech Technical University in Prague, Faculty of Mechanical Engineering, Department of Production Machines and Equipment, RCMT, Horská 3, 128 00 Prague, Czech Republic*

martin.mares@rcmt.cvut.cz

Abstract
Thermally induced errors are a dominant source of machine tool (MT) inaccuracy and are often among the most difficult to mitigate. Software compensation of thermally induced displacements at the tool contact point (TCP) is therefore widely used; however, an extensive set of measured data is typically required to calibrate such models. When a compensation model is intended to be valid across the entire workspace of a large machine tool (such as horizontal milling centre; the target machine in this research), a dense grid of measurement configurations is often needed, making experimental analysis costly and time-consuming. This paper builds on previous research in which a whole-machine finite element analysis (FEA) model was used to identify the spatial dependence of thermal volumetric errors on machine-axis configuration and to select a small set of critical axis positions for targeted experiments. The main contribution of the present paper is the development of a continuously re-tunable, spatially dependent thermal error compensation model trained only on data from these FEA-informed sparse experimental setups. The proposed concept reduces the number of required experiments, thereby minimising machine downtime for thermal characterisation, reducing energy consumption, and lowering the overall cost of developing robust thermal error compensation models. The effectiveness of the approach is demonstrated on experimental data obtained in an additional, generally selected axis configuration used for validation.

Machine tool, Finite element analysis (FEA), Volumetric error, Thermal error compensation

1. Introduction

Machine tools (MT) are loaded during operation by several physical phenomena that cause structural deformations, such as vibrations, chatter, gravitational effects, and thermal loads. Geometric errors resulting from non-stationary thermal phenomena manifest as deviations between the desired and the actual relative motion of the tool and the workpiece. Thermal errors are reported to account for 40–70% of the total MT inaccuracy [1]. Consequently, reducing thermally induced errors has long been a key objective for MT designers and control engineers.

Mitigation approaches can be broadly divided into three groups [2]:

- design measures that reduce sensitivity to heat flux (e.g., thermally symmetric structures, thermal insulation),
- control of the machine and environmental temperatures (e.g., cooling systems and environmental control), and
- thermal error compensation in the control system.

This paper presents an FEA-informed compensation strategy (Figure 1) that combines: 1\ analysis of the thermal behaviour of a horizontal milling centre (target machine) using a spatially reconfigurable finite element model (FEM) to identify the most influential machine-axis configurations, 2\ targeted experiments performed only in these critical configurations, and 3\ development of a continuously tunable volumetric compensation model based on thermal transfer functions (TTF) formulated in a state-space representation.

The proposed concept reduces the number of measurement configurations required during the experimental phase, thereby shortening machine occupancy time and lowering the overall cost of thermomechanical characterisation, while enabling robust compensation of spatially dependent thermal errors particularly relevant for heavy-duty machine tools. The effectiveness of the concept is demonstrated by compensating thermally induced displacements in the *Y* direction of the target machine.

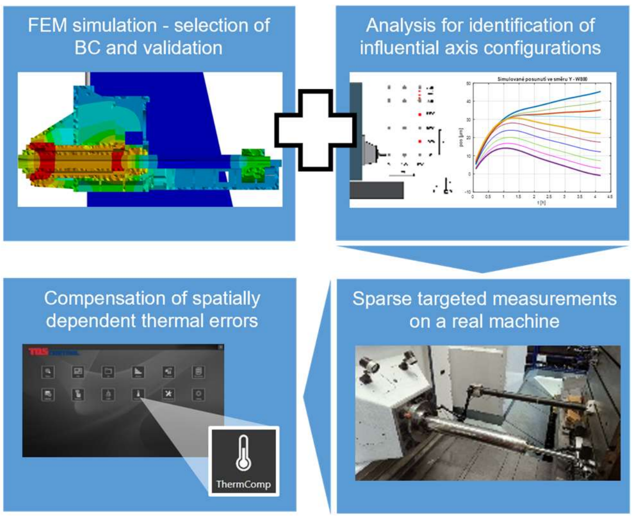

Figure 1. Value chain of the FEA-informed compensation concept

2. Simulation, analysis and measurement

In the preceding study [3], the thermal behaviour of the target machine (Figure 2) was analysed using a whole-machine FEA model with the aim of predicting thermally induced volumetric displacements at the TCP across the workspace without extensive experimental campaigns. The FEA model included the main structural components; drives were represented by lumped masses and/or equivalent springs. Spindle bearings were modelled using equivalent stiffness and thermal boundary conditions (BC) derived from bearing losses. Forced and free convection, as well as radiation, were applied to external surfaces.

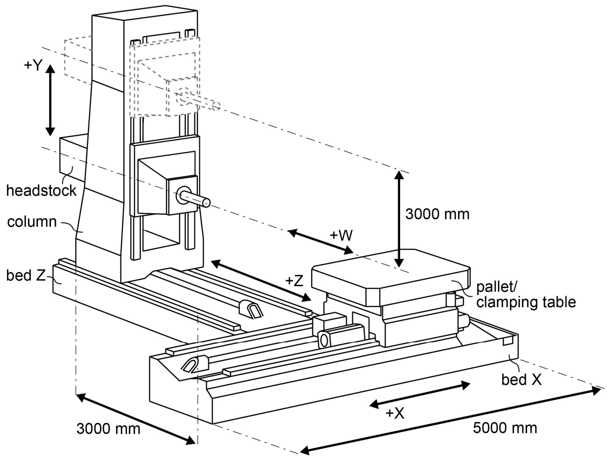

Figure 2. Kinematic description of target machine - horizontal milling centre with a moving table

Simulations were performed for a grid of 18 positions in the *YZ* plane under a constant thermal load corresponding to spindle rotation at 4000 rpm. Displacement at TCP was evaluated after four hours of loading, i.e., after approximate thermal stabilisation. The results showed that the largest absolute thermal error occurs in the *Z* direction, but with only minor variation across the *Y*-axis travel. In contrast, displacements in the *Y* direction showed a strong dependence on *Y*-axis position and exhibited different time trends in different parts of the *Y*-axis stroke. The influence of the *W*-axis (spindle extension) was found to be linear.

Based on the simulated displacement fields, five representative measurement configurations were selected to capture the most critical thermal trends, reducing the number of experimental configurations from 18 to 5 (Figure 3). Subsequent measurements at these configurations — under the same spindle load conditions and in a stable ambient environment (the target machine was located in the manufacturer's prototype & testing hall) — confirmed that, although the absolute deformation magnitudes differ between the FEA model and the experiments, the FEA model reproduces the qualitative trends sufficiently well for the purpose of experiment design.

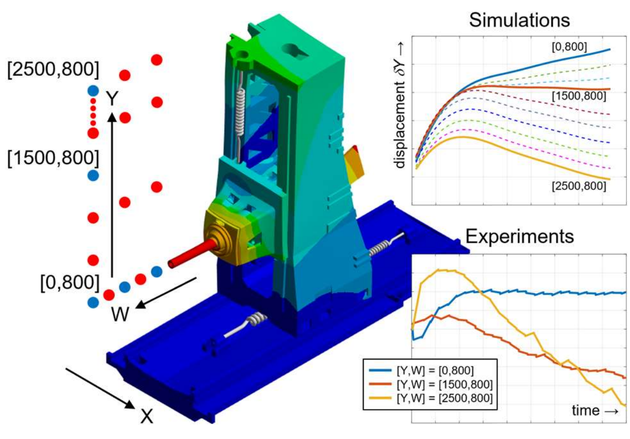

Figure 3. Identified measurement configurations (blue dots), FEA results (upper chart), and experimental verification of *Y*-direction displacements for three configurations along the *Y*-axis: [Y,W] = [0,800], [1500,800], and [2500,800] (lower chart)

The study [3] further indicated that a single global compensation function is inadequate; instead, the workspace should be partitioned into zones, each described by its own sub-model. The present paper builds on these findings by developing and evaluating a spatially dependent compensation model and an interpolation strategy that enables continuous compensation across the workspace.

3. Compensation strategy

The compensation strategy proposed in this paper focuses on thermally induced displacements in the *Y* direction (δY) caused by spindle rotation (only heating phases; left part of Figure 4). As shown in Figure 3, δY depends strongly on *Y*-axis position and exhibits varying time responses along the *Y*-axis stroke. In contrast, the selected model input — measured temperature difference at the rear spindle bearings — shows a similar time evolution in all calibration experiments (right part of Figure 4). This supports the use of a common thermal excitation signal combined with spatially dependent sub-models.

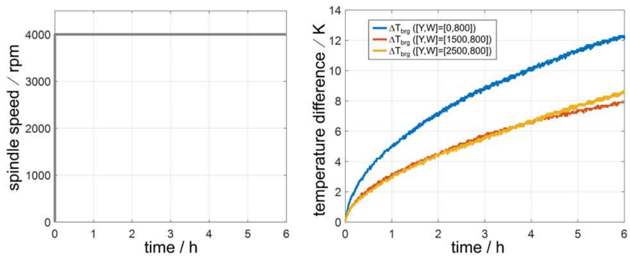

Figure 4. Spindle speed profile (left) and measured temperature difference at spindle rear bearings (right) during FEA-informed calibration experiments

As suggested by [3], the workspace is divided into zones described by locally calibrated sub-models. A continuous compensation function over the full stroke is then obtained by interpolating between these sub-models.

3.1. Sub-model identification in critical axis configurations

System identification theory is used to construct dynamic thermal error compensation sub-models for the FEA-identified critical axis configurations. The thermal transfer function (TTF) approach reflects basic heat transfer principles, which makes calibration of empirical parameters straightforward. The applicability of TTF-based compensation has been verified on various MT structures, equipment, and technologies in [4] and [5]. In discrete form, a TTF describes the relationship between excitation (temperature) and response (displacement):

$$y(t) = \varepsilon . u(t) + e(t) = \frac{a_n z^{-n} + \cdots + a_1 z^{-1} + a_0 z^0}{b_m z^{-m} + \cdots + b_1 z^{-1} + b_0 z^0} u(t) + e(t), \quad (1)$$

where *u(t)* is the input and *y(t)* is the output vector, *ε* represents the TTF in the time domain, *e(t)* is a disturbance term (further neglected), *z* is the complex variable, *n* is the numerator order, *m* is the denominator order ($m > n$), and $a_{0:n}$ and $b_{0:m}$ are calibration coefficients. The difference equation form in the time domain is given in:

$$y(k) = \frac{u(k-n)a_n + \cdots + u(k-1)a_1 + u(k)a_0 - y(k-m)b_m - \cdots - y(k-1)b_1}{b_0}, \quad (2)$$

where $k-n$ ($k-m$) represents an *n*-step (*m*-step) delay at the sampling frequency. Linear parametric ARX (autoregressive with exogenous input) structures are identified in MATLAB® [6].

The basis of the compensation model is formed by three TTFs calibrated in the critical configurations [Y,W] = [0,800], [1500,800], and [2500,800]. The sub-models are expressed as:

$$\begin{aligned} \delta Y_{[0,800]} &= \Delta T_{brg} \cdot \varepsilon_{[0,800]} \\ \delta Y_{[1500,800]} &= \Delta T_{brg} \cdot \varepsilon_{[1500,800]} \\ \delta Y_{[2500,800]} &= \Delta T_{brg} \cdot \varepsilon_{[2500,800]}, \end{aligned} \tag{3}$$

where $\delta Y_{[0,800]:[2500,800]}$ are the model-predicted TCP displacements, ΔT_{brg} is the measured rear spindle bearing temperature difference, and $\varepsilon_{[0,800]:[2500,800]}$ are the TTFs representing the spindle thermal influence in the three calibration configurations. Figure 5 compares measured displacements (solid lines) and TTF predictions (dashed lines) for the calibration experiments; the residuals are shown in the right plot.

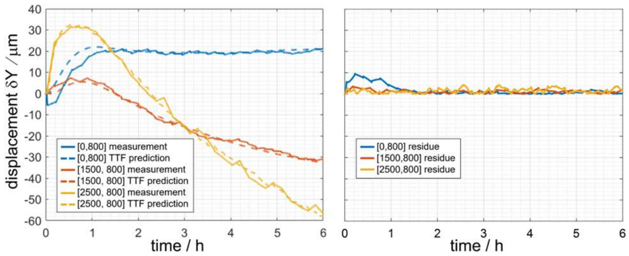

Figure 5. Measured and predicted (left) and residual (right) thermally induced *Y*-direction displacements during FEA-informed calibration experiments

Using the RMSE criterion, the sub-models reduce thermally induced displacement by 51%, 89%, and 93% for [Y,W] = [0,800], [1500,800], and [2500,800] configurations respectively, during the calibration experiments.

3.2. Spatially dependent compensation model (state-space interpolation)

To enable continuous compensation during motion along the Y-axis, the locally identified sub-models must be smoothly interpolated. A direct LPV (linear parameter-varying) formulation, where model parameters depend on the current *Y* position, may suffer from stability issues when parameters vary, even if each local model is stable [7]. To address this, interpolation is performed in state space [8], which preserves the internal dynamics and supports stable transitions between sub-models.

Therefore, each TTF sub-model in equation (3) is converted into the following state-space form:

$$\begin{aligned} \dot{x}(t) &= Ax(t) + Bu(t) \\ y(t) &= Cx(t) + Du(t), \end{aligned} \tag{4}$$

where $x(t)$ is the state vector, $\dot{x}(t)$ is the state derivative, $y(t)$ is the output, $u(t)$ is the input (control), and A, B, C, D are the system matrices. A detailed conversion procedure is given in [9].

Extension of the compensation model over the full *Y*-axis stroke is achieved using position-dependent weights. First, an inverse-distance value $v_{[Y,W]}$ from each calibration position is computed:

$$\begin{aligned} v_{[0,800]} &= |0 - Y_{actual}|^{-1} \\ v_{[1500,800]} &= |1500 - Y_{actual}|^{-1} \\ v_{[2500,800]} &= |2500 - Y_{actual}|^{-1}, \end{aligned} \tag{5}$$

where Y_{actual} is the current *Y*-axis coordinate. Second, normalisation yields the weights $w_{[Y,W]}$ for each sub-model:

$$\begin{aligned} w_{[0,800]} &= \frac{v_{[0,800]}}{v_{[0,800]}+v_{[1500,800]}+v_{[2500,800]}} \\ w_{[1500,800]} &= \frac{v_{[1500,800]}}{v_{[0,800]}+v_{[1500,800]}+v_{[2500,800]}} \\ w_{[2500,800]} &= \frac{v_{[2500,800]}}{v_{[0,800]}+v_{[1500,800]}+v_{[2500,800]}}, \end{aligned} \tag{6}$$

where the following applies:

$$w_{[0,800]} + w_{[1500,800]} + w_{[2500,800]} = 1. \tag{7}$$

The resulting volumetric compensation model in state-space form for an arbitrary *Y* position at full *W*-axis extension (W = 800 mm) is defined as a weighted combination of the sub-models:

$$\begin{aligned} \dot{x}(t) &= A_{[Y,800]}x(t) + B_{[Y,800]}u(t) \\ y(t) &= C_{[Y,800]}x(t) + D_{[Y,800]}u(t), \end{aligned} \tag{8}$$

where:

$$\begin{aligned} A_{[Y,800]} &= A_{[0,800]} \cdot w_{[0,800]} + A_{[1500,800]} \cdot w_{[1500,800]} + \\ &\quad + A_{[2500,800} \cdot w_{[2500,800]} \\ B_{[Y,800]} &= B_{[0,800]} \cdot w_{[0,800]} + B_{[1500,800]} \cdot w_{[1500,800]} + \\ &\quad + B_{[2500,800} \cdot w_{[2500,800]} \\ C_{[Y,800]} &= C_{[0,800]} \cdot w_{[0,800]} + C_{[1500,800]} \cdot w_{[1500,800]} + \\ &\quad + C_{[2500,800} \cdot w_{[2500,800]} \\ D_{[Y,800]} &= D_{[0,800]} \cdot w_{[0,800]} + D_{[1500,800]} \cdot w_{[1500,800]} + \\ &\quad + D_{[2500,800} \cdot w_{[2500,800]} \end{aligned} \tag{9}$$

and

$Y \in \langle 0,2500 \rangle$.

4. Concept verification

To verify the concept defined by equations (8) and (9), a validation point was selected in the *YW* plane corresponding to the axis configuration [Y,W] = [2100,200]. The location of this point within the workspace is schematically indicated by the purple dot in the left part of Figure 6.

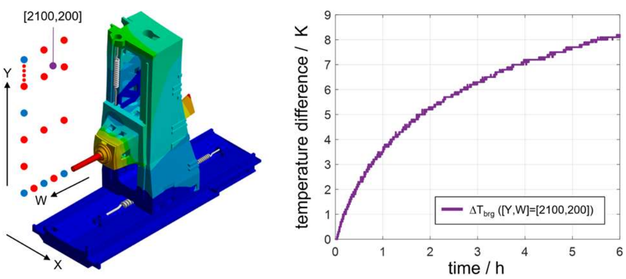

Figure 6. Visualisation of verification configuration [Y,W]=[2100,200] (left) and measured rear spindle bearing temperature difference during the verification experiment (right)

The TTF-based compensation model (equations (8) and (9)) is calibrated for *W* = 800 mm and reliably approximates thermally induced displacements along the *Y*-axis stroke at this full *W*-axis extension. The FEA results in [3] further indicate a linear dependence of the thermomechanical response along the *W*-axis stroke. Based on this assumption, an FEA-derived scaling factor was determined to account for the changed *W* position (*W* = 200 mm). The factor equals 0.7 and is applied to the model output to approximate measured displacements in the validation configuration [Y,W] = [2100,200], without additional calibration experiments.

The validation experiment was performed under conditions comparable to the calibration tests: the spindle speed followed the profile shown in Figure 4 (left), and the measured variation of the model input temperature during the validation test is shown in Figure 6 (right).

Figure 7 shows the measured displacements (solid line) and the model predictions (dashed line) for the validation experiment; residuals are shown in the right plot. The residual corresponds to the remaining thermal error after compensation by the spatial model (equations (8) and (9)) with the additional *W*-axis scaling factor of 0.7.for the extension of the *W*-axis corresponding to 200 mm.

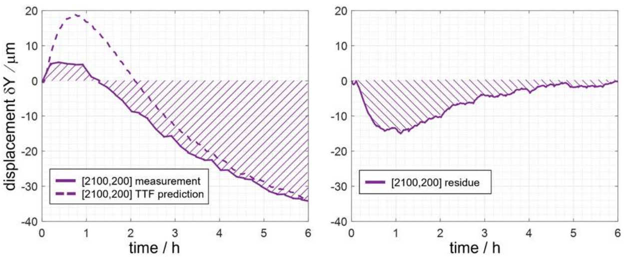

Figure 7. Measured and predicted (left) and residual (right) thermally induced *Y*-direction displacements during the verification experiment

Using the RMSE criterion, the proposed compensation model achieves a 52% reduction of thermally induced *Y*-direction displacement in the general verification configuration [Y,W] = [2100,200].

5. Conclusions

This paper presented an FEA-informed workflow for efficient identification and compensation of spatially dependent thermal volumetric effects in a horizontal milling centre. Building on earlier whole-machine FEA results used to reveal the dependence of thermal errors on machine-axis configuration, the approach uses FEA to select a small number of critical measurement configurations and performs targeted experiments only in these configurations. Local dynamic sub-models were identified using thermal transfer functions (TTF), and a continuous compensation model across the *Y*-axis stroke was obtained by interpolating the sub-models in a state-space representation.

The main findings can be summarised as follows. (i) Whole-machine FEA is effective for identifying axis configurations that exhibit significantly different thermal responses, enabling an experiment plan that captures the dominant spatial trends with a reduced number of measurements. (ii) The locally calibrated TTF sub-models achieved substantial reduction of thermally induced *Y*-direction displacement in the calibration configurations. (iii) State-space interpolation provides a practical way to achieve smooth, continuous compensation across the workspace while mitigating stability issues associated with direct parameter interpolation. The concept was validated in an additional axis configuration not used for calibration. By combining the spatial model with an FEA-derived *W*-axis scaling factor, the model reduced the validation displacement by 52% without additional calibration experiments.

Future work will focus on refining the *W*-axis dependency to quantify potential non-linearities, evaluating robustness under varying spindle speed profiles, ambient conditions, cooling etc. and verify the concept on different types of machines.

Acknowledgement

This research has received funding from the Technology Agency of the Czech Republic (Project TN02000018 - National Centre of Competence ENGINEERING). The work was also supported by the Grant Agency of the Czech Technical University in Prague, grant no. SGS25/135/OHK2/3T/12.

References

[1] Mayr J. et al. 2012 Thermal issues in machine tools. CIRP Annals **61**: 771–791.

[2] Weck M. et al. 1995 Reduction and Compensation of Thermal Errors in Machine Tools. *Annals of the CIRP* **44** (2) 589-598

[3] Divíšek D. et al. 2025 Analysis of Thermal Volumetric Effect on Machine Structure Using FEA Model. *In: euspen's Special Interest Conference: Precision & Performance, Cranfield, United Kingdom,* 53-56, ISBN: 978-0-9957751-6-9

[4] Horejš O. et al. 2022 Compensation of thermally induced errors in five-axis computer numerical control machining centers equipped with different spindles, J. Manuf. Sci. Eng., **144** (10)

[5] Mareš M. et al. 2019 Thermal Error Minimization of a Turning-Milling Center with Respect to its Multi-Functionality, *International Journal of Automation Technology* **14** (3), 475-483

[6] Ljung L L. 2015 System Identification Toolbox™ User's Guide, *The MathWorks*

[7] Toth, R. et al. 2007 Discrete time LPV I/O and state-space representations, differences of behavior and pitfalls of interpolation, *In: Proceedings of the European Control Conference, Kos, Greece,* 5418-5425, ISBN: 978-960-89028-5-5

[8] Chen X. 2021 Lecture on State-Space Representations, *available: https://faculty.washington.edu/chx/teaching/me547/1-6_ss_realization.pdf*

[9] https://www.mathworks.com/help/releases/R2024b/control/ref/ss.html?browser=F1help